



Research Article

Energetic and exergetic performance comparison of an experimental automotive air conditioning system using refrigerants R1234yf and R134a

Alpaslan ALKAN^{1,*}, Ahmet KOLIP¹, Murat HOSOZ²

¹Department of Mechanical Engineering, Sakarya University of Applied Sciences, Sakarya, Turkey

²Department of Automotive Engineering, Kocaeli University, Kocaeli, Turkey

ARTICLE INFO

Article history

Received: 03 December 2019

Accepted: 29 February 2020

Key words:

R1234yf; R134a; Automotive;
Air conditioning; Refrigeration;
Performance

ABSTRACT

In this study, the energetic and exergetic performance merits of an automotive air conditioning (AAC) system using R134a and R1234yf have been investigated. For this aim, a laboratory AAC system was developed and equipped with devices for mechanical measurements. The refrigeration circuit of the system mainly had an evaporator, condenser, liquid receiver, fixed capacity compressor, and thermostatic expansion valve. The tests were performed by changing the compressor speed and air stream temperatures incoming the condenser and evaporator. Based on energy and exergy analysis, various performance parameters of the AAC system for both refrigerants were determined and presented in comparative graphics. It was found that R1234yf resulted in 0.4–10.9% lower refrigeration capacity, 5.5–11.6% lower COP, and 4.7–16.1°C lower compressor discharge temperature, while yielding 9.3–22.3% higher refrigerant mass flow rate and 1.1–3.5°C higher conditioned airstream temperature in comparison to R134a. Moreover, the components of the R1234yf system usually destructed more exergy, and the total exergy destruction rate per unit refrigeration capacity of the R1234yf system was 4.1–15.3% greater than that of the R134a one.

Cite this article as: Alkan A, Kolip A, Hosoz M. Energetic and exergetic performance comparison of an experimental automotive air conditioning system using refrigerants R1234yf and R134a. J Ther Eng 2021;7(5):1163–1173.

INTRODUCTION

Cars equipped with air conditioning systems first appeared in the 1930s after the development of Chlorofluorocarbon group refrigerants. Because refrigerants

containing chlorine caused depletion of the atmospheric ozone layer, their use was restricted by the Montreal Protocol in 1987. Consequently, manufacturers started to employ R134a, a refrigerant from Hydrofluorocarbon (HFC) group,

*Corresponding author.

*E-mail address: aalkan@subu.edu.tr, akolip@subu.edu.tr, mhosoz@kocaeli.edu.tr

This paper was recommended for publication by Dr. Pouria Ahmadi



as a substitute for R12 in automotive air conditioning (AAC) systems. Then, raising attention to global warming led to the approval of the Kyoto Protocol in 1997 as a step for solving this problem by controlling gases with high global warming potential (GWP). Consequently, due to their high GWP values, the use of refrigerants in the HFC group was first restricted, and then they were gradually banned. In accordance with the Kyoto Protocol, European Union issued an updated F-gas Regulation prohibiting the use of refrigerants having GWP values over 150 in the AAC systems of vehicles put on the EU market after January 1st, 2017 [1]. Because R134a has a GWP of 1430, the automotive industry has been seeking alternative refrigerants which obey the limitations yet providing satisfactory performance. Refrigerants considered as alternatives to R134a in AAC systems are CO₂ and two recently developed refrigerants from Hydrofluoroolefin (HFO) group, namely R1234yf and R1234ze [2]. CO₂ has extremely high compressor discharge pressures leading to heavy equipment and yields a relatively low coefficient of performance (COP). With a GWP of only 4 and higher energy effectiveness compared to R1234ze, R1234yf is presently considered as the best substitute for R134a, although it has mild flammability as listed in A2L classification [2, 3].

After the development of R1234yf, many investigations have been carried out to determine its performance in various vapour-compression refrigeration (VCR) and air conditioning (AC) systems. Lee and Jung [4] investigated the experimental performance of an AC system for R1234yf and R134a, concluding that the R1234yf system had 2.7% lower COP and 4% less cooling capacity relative to the R134a one. Navarro-Esbri et al. [5] performed tests on a VCR system and found that the system with R1234yf had 9% less cooling capacity and 19% lower COP in comparison to the system with R134a. Navarro et al. [6] performed comparative tests of a bus air conditioning system using R1234yf, R134a, and R290, and determined that R1234yf yielded a lower COP and about 10°C lower compressor discharge temperatures than the other two refrigerants. Mota-Babiloni et al. [7] determined that a VCR system with R1234yf provided on average 9% lower cooling capacity and 7% less COP in comparison to the one with R134a. However, the R1234yf system yielded COP values close to those in the R134a one when an internal heat exchanger (IHx) was employed between the suction and liquid lines of the refrigeration circuit. Daviran et al. [8] simulated an AAC system with R1234yf and found that R1234yf yielded 1.3–5.0% lower COP than R134a for a constant cooling capacity. Direk et al. [9] evaluated the experimental drop-in performance of R1234yf in an AAC system employing an IHx. Although the cooling capacity and COP of the R1234yf system were on average 17.1% and 12.4% less than those of the R134a one, respectively, they were improved on average 7.9% and 4.1%, respectively, when an IHx was employed. Wantha [10] investigated the overall heat transfer coefficient of an IHx and its effects on the COP of a VCR system using

R134a and R1234yf. He found that the use of IHx increased COP by 3.78% and 2.11%, for R1234yf and R134a, respectively. Aral et al. [11] developed two different empirical correlations to predict the steady-state performance of an experimental AAC system using R134a and R1234yf, and confirmed their accuracy with experimental data.

In addition to the first law analysis, some investigations have dealt with exergy analysis of AAC systems employing alternative refrigerants to pinpoint the components causing thermodynamic inefficiency. Yataganbaba et al. [12] conducted a theoretical exergy analysis of a vapour-compression refrigeration system employing R1234yf and R1234ze as alternatives to R134a. They found that the exergetic efficiency of the R1234ze system was comparable to the R134a one, while the R1234yf system yielded significantly lower exergetic efficiency. Cho and Park [13] determined that an AAC system with R1234yf yielded 4.0–7.0% lower cooling capacity, 3.6–4.5% less COP, and 3.4–4.6 lower second law efficiency relative to the system with R134a. In their theoretical analysis of an AAC system for R134a and R1234yf, Golzari et al. [14] found that R1234yf had a higher exergetic efficiency, and the compressor was the component causing maximum exergy destruction. Devencioglu and Oruc [15] theoretically studied the COP and exergetic efficiency of various VCR systems using R1234yf, R1234ze, R513a, R445a, and R450a as alternatives to R134a. They found that R450a yielded almost as high COP values as R134a, and R445a resulted in the highest exergetic efficiency. Chopra et al. [16] compared the theoretical energetic and exergetic performance of R134a and its various alternatives including R1234yf in a two-stage VCR system. They determined that R1234yf had a lower exergy efficiency and higher exergy destruction compared to R134a. Agarwal et al. [17] theoretically investigated the effect of sub-cooling on the energetic and exergetic performance of a VCR system for refrigerants R134a, R1234yf, and R1234ze. They found that sub-cooling promoted COP and exergetic efficiency, and R1234ze performed better than R1234yf and comparable to R134a.

As seen in the literature survey outlined above, only the energetic performance parameters of the systems were usually compared in the investigations on the experimental performance of AAC systems using R134a and R1234yf. Moreover, the comparisons were made using test results collected in a narrow range of operating conditions. As a contribution to the literature, this study presents an experimental comparison of not only energetic but also exergetic performance parameters of an AAC system for both refrigerant cases, which allows pinpointing the components causing lower performance for each refrigerant. Furthermore, the performance comparisons were made using test data acquired in a broader range of operating conditions. In this study, the performance evaluation was made in terms of the refrigerant mass flow rate, conditioned air temperature, refrigeration capacity, compressor power, COP, discharge temperature, component exergy destruction rates, and

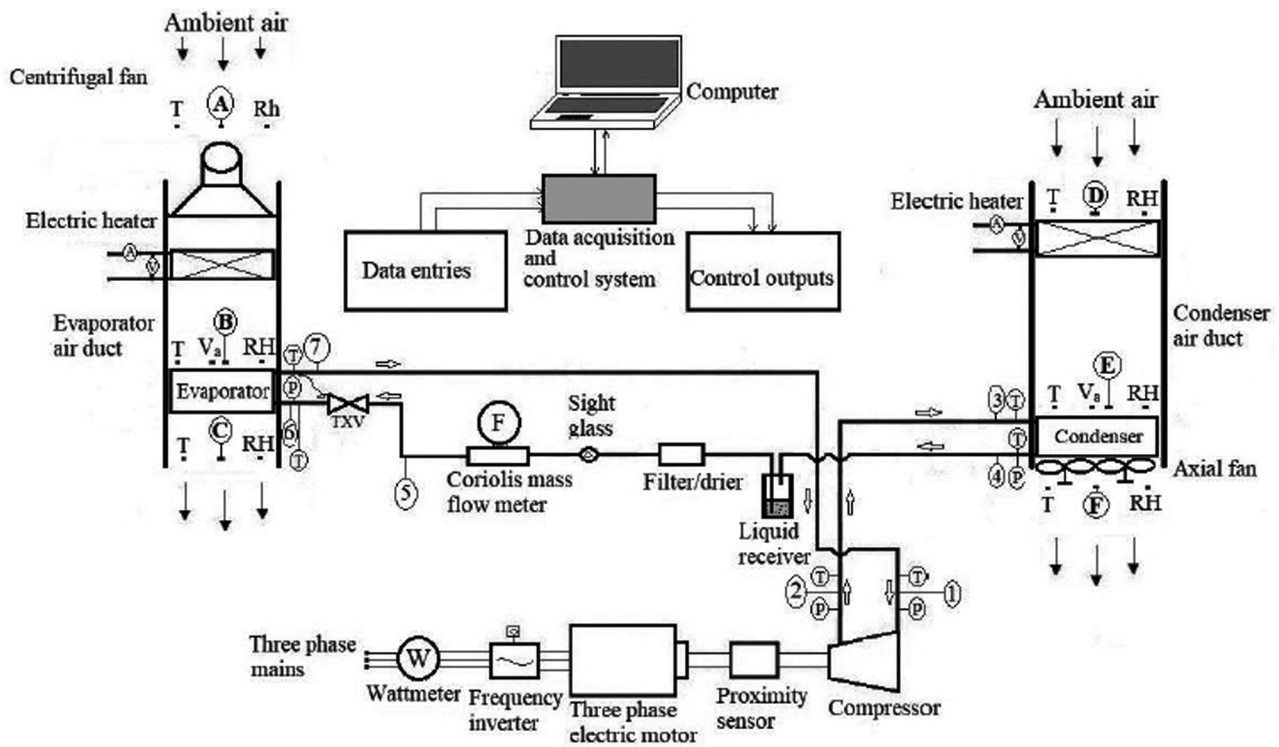


Figure 1. Sketch of the experimental AAC system.

the rate of total exergy destruction per unit refrigeration capacity.

EXPERIMENTAL SYSTEM AND TESTING PROCEDURE

The sketch of the experimental system is indicated in Figure 1. It consists of the AAC system components employed in a compact automobile, namely a fixed-capacity wobble-plate compressor, parallel-flow micro-channel condenser, laminated evaporator, TXV, liquid receiver, and filter/drier. Technical specifications of these components are reported in Table 1.

The compressor was operated by a 5.5 kW three-phase asynchronous electric motor through a belt-pulley mechanism. A frequency inverter was employed to energise the motor so that the compressor could be operated at the required speeds. The evaporator and condenser were placed in air ducts containing electric heaters to obtain the desired airstream temperatures entering these two components. The heating capacities of the condenser and evaporator duct heaters were 5.4 and 1.8 kW, respectively. A condenser airstream at an average speed of 3.6 m s⁻¹ was provided by a twin axial fan arrangement, while an evaporator airstream at an average speed of 3.6 m s⁻¹ was provided by a centrifugal fan as shown in Figure 1.

Measurements of physical variables such as pressure, temperature, relative humidity, airspeed, compressor

Table 1. Technical specifications of the components

Component	Specifications
Compressor	Seven-cylinder, wobble-plate, fixed capacity type Stroke volume: 154.9 cc rev ⁻¹
Condenser	Parallel-flow, micro-channel type Dimensions: 630 mm × 380 mm × 20 mm Number of channels: 37
Evaporator	Laminated type Dimensions: 235 mm×220 mm×65 mm Number of channels: 20
Expansion device	Internally balanced thermostatic expansion valve Capacity: 5.5 kW

speed, and refrigerant flow rate were performed at the points shown in Figure 1. A Coriolis mass flow meter was employed to measure the refrigerant flow rate in the system. The evaporator and condenser pressures were measured by both pressure transmitters and Bourdon manometers at the points indicated by the symbol P in Figure 1. Type T thermocouples measured the refrigerant temperatures at the points indicated by the symbol T. The air dry-bulb temperatures and relative humidity were measured by SHT 71 type temperature/humidity sensors at the points in the air ducts indicated by the symbols T and RH, respectively.

Table 2. Specifications of the measurement devices

Physical quantity	Device	Range	Accuracy
Refrigerant temperature	Type T thermocouple	−40/350°C	±0.5°C
Air dry bulb temperature	SHT 71 temperature sensor	−40/123°C	±0.4°C
Pressure	Vika S−10 transmitter	0/25 bar	0.25 bar
Relative humidity	SHT 71 humidity sensor	0/100%	±3%
Air velocity	EE65−VCK200 transmitter	0.2/10 m s ^{−1}	±0.2 m s ^{−1}
Mass flow rate	Krohne Optimass 3300C H04 Coriolis flow meter	0/450 kg h ^{−1}	±0.1%

The average airspeeds in the ducts were measured by air-flow transmitters at the points shown by the symbol V_a . The sensors of these transmitters were located at the proper positions so that they could measure the average speeds. The speed of the compressor pulley was measured by an inductive proximity sensor. Digital and analogue data from the sensors were collected by data acquisition systems and transmitted to a computer via an RS485 MODBUS communication protocol. The values of the desired operating conditions were specified by the user in the computer environment, and the operation of the experimental system at the desired conditions was accomplished by a PLC, which could change the compressor speed and air temperatures entering the evaporator and condenser by controlling the frequency inverter of the compressor electric motor and duct electric heaters, respectively. The basic specifications of the measurement devices are provided in Table 2. The photographs of the experimental system taken from two different perspectives are indicated in Figure 2, and a scheme showing the connections among the components of the instrumentation and control system is indicated in Figure 3. Further information on the experimental system, which was developed within a doctoral study, can be found in Alkan [18].

The refrigerants tested in the experimental AAC system were R134a and R1234yf. Utilising Refs [7] and [15], various thermodynamic, environmental, and safety properties of these refrigerants are reported in Table 3. The first group of tests was conducted with an R134a charge of 1500 g, which provided the optimum system performance. Then, the R134a was recovered and, in accordance with the literature [19], 1350 g of R1234yf, 10% less than the R134a charge, was employed in the system for the second group of tests. The difference between the R134a and R1234yf charges stems from the fact that the liquid density of R1234yf is about 10% less than that of R134a. The

Table 3. Thermodynamic, environmental and safety properties of the tested refrigerants

Refrigerant	R134a	R1234yf
Chemical formula	C ₂ H ₂ F ₄	C ₃ H ₂ F ₄
Molecular weight (kg/kmol)	102	114
Boiling point at 101.325 kPa (°C)	−26.07	−29.45
Critical temperature (°C)	101.06	94.70
Critical pressure (kPa)	4059	3382
Liquid density at 0°C (kg/m ³)	1294.8	1176.3
Vapour density at 0°C (kg/m ³)	14.428	17.6
Latent heat of vapourisation at 0°C (kJ/kg)	198.60	163.29
ODP	0	0
GWP	1430	4
ASHRAE Safety Group	A1	A2L

system was tested for the same air temperatures incoming the condenser and evaporator, namely 27°C and 37°C. For the air inlet temperature of 27°C, the compressor speed was changed from 800 rpm to 1600 rpm with 200 rpm intervals. For this air inlet temperature, extremely low evaporator temperatures were experienced when the compressor speed exceeded 1600 rpm, which led to the evaporator surface temperatures below 0°C and frost formation on the evaporator surface. Therefore, the 27°C tests were conducted for the compressor speeds up to 1600 rpm. Moreover, the air relative humidity incoming the evaporator was maintained at 40±4% for both refrigerants in 27°C air inlet temperature tests. For the air inlet temperature of 37°C, frost formation on the evaporator surface was not observed at elevated speeds due to rising evaporating temperature. Therefore, tests up to 2800 rpm were conducted for this air inlet temperature. Furthermore, the relative humidity of the air stream incoming the evaporator was maintained at 24±4% for both refrigerants in 37°C air inlet temperature tests. Before starting a test, the desired compressor speed and air stream temperatures incoming the condenser and evaporator were specified to the control software of the PLC, which operated the system in accordance with these inputs. The performance of the experimental system was evaluated using only steady-state data, which were collected between the 10th and 15th mins of a test.

ENERGY AND EXERGY ANALYSIS OF THE EXPERIMENTAL SYSTEM

The conservation of energy principle can be applied to the components of the experimental AAC system to evaluate its energetic performance parameters. In this analysis, it is assumed that the kinetic and potential energies do not change in each component, and the pressure drops in the evaporator, condenser, and refrigerant lines are negligible.



Figure 2. Photographs of the experimental AAC system; (a) Front view, (b) Rear view.

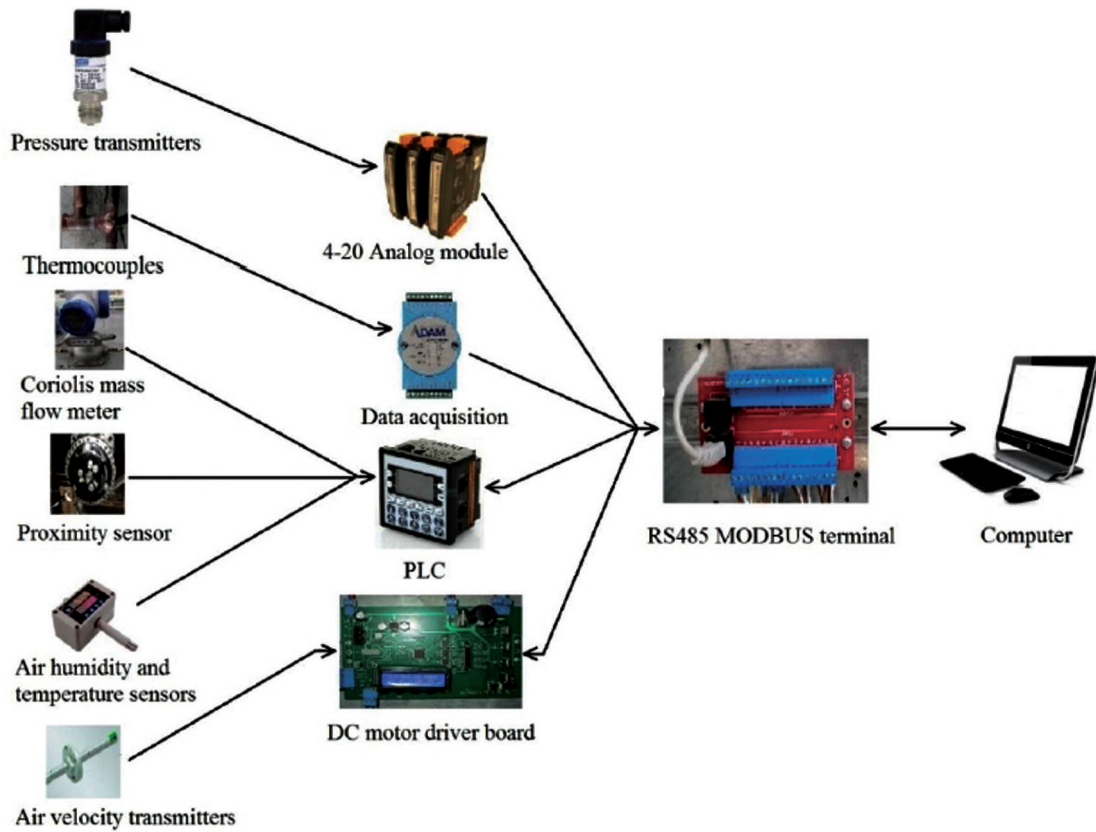


Figure 3. Schematic view of the connections in the instrumentation and control system.

By using the refrigerant mass flow rate and refrigerant enthalpies at the inlet and outlet of the evaporator, the refrigeration capacity can be evaluated from

$$\dot{Q}_{evap} = \dot{m}_r (h_7 - h_6) \quad (1)$$

In this study, REFPROP 9.1 software was used to determine the enthalpy and entropy of the refrigerants as functions of pressure and temperature measurements.

Assuming that the compressor is adiabatic, the power of compression transferred to the refrigerant can be determined from

$$\dot{W}_{comp} = \dot{m}_r (h_2 - h_1) \quad (2)$$

An indicator of the energy effectiveness of a refrigeration circuit is its COP, which is the refrigeration capacity per unit compressor power, i.e.,

$$COP = \frac{\dot{Q}_{evap}}{\dot{W}_{comp}} \quad (3)$$

The thermodynamic inefficiency of the components of the AAC system can be revealed by performing an exergy analysis. For control volumes, the general form of steady-state exergy rate balance equation can be expressed as [20–22]

$$\sum \left(1 - \frac{T_o}{T_j} \right) \dot{Q}_j + \sum \dot{m}_{in} \psi_{in} = \sum \dot{m}_{out} \psi_{out} + \dot{W}_{cv} + \dot{E}x_d \quad (4)$$

where $\dot{E}x_d$ indicates the exergy destruction rate and ψ is the specific flow exergy of the refrigerant that can be determined from

$$\psi = (h - h_o) - T_o (s - s_o) \quad (5)$$

where subscript “0” denotes dead state. The expressions for the exergy destruction rate in each component of the AAC system are obtained from Eq. (4), and listed in Table 4. In these expressions, $\dot{m}_{a,cond}$ and $\dot{m}_{a,evap}$ stand for the air mass flow rates passing over the condenser and evaporator, respectively. Moreover, the specific flow exergies of air at the points B, C, E, and F can be determined from [23, 24]

$$\begin{aligned} \psi_a = & (c_{p,a} + \omega c_{p,v}) T_o \left[\left(\frac{T}{T_o} \right) - 1 - \ln \left(\frac{T}{T_o} \right) \right] \\ & + \left[\left(1 + 1.6078\omega \right) R_a T_o \ln \left(\frac{P}{P_o} \right) \right] \\ & + R_a T_o \left\{ \left(1 + 1.6078\omega \right) \ln \left(\frac{1 + 1.6078\omega_o}{1 + 1.6078\omega} \right) \right. \\ & \left. + 1.6078\omega \ln \left(\frac{\omega}{\omega_o} \right) \right\} \end{aligned} \quad (6)$$

Table 4. The exergy destruction rates of the AAC system components

Component	Expression
Compressor	$\dot{E}x_{d,comp} = \dot{m}_r (\psi_{comp,in} - \psi_{comp,out}) + \dot{W}_{comp}$
Condenser	$\dot{E}x_{d,cond} = \dot{m}_r (\psi_{cond,in} - \psi_{cond,out}) + \dot{m}_{a,cond} (\psi_E - \psi_F)$
Expansion valve	$\dot{E}x_{d,TV} = \dot{m}_r (\psi_{TV,in} - \psi_{TV,out})$
Evaporator	$\dot{E}x_{d,evap} = \dot{m}_r (\psi_{evap,in} - \psi_{evap,out}) + \dot{m}_{a,evap} (\psi_B - \psi_C)$

Finally, the rate of total exergy destruction in the AAC system can be obtained from

$$\dot{E}x_{d,tot} = \dot{E}x_{d,comp} + \dot{E}x_{d,cond} + \dot{E}x_{d,TV} + \dot{E}x_{d,evap} \quad (7)$$

UNCERTAINTY ANALYSIS

In order to calculate the uncertainties for the performance parameters of the AAC system, the method proposed by Moffat [25] was used. According to this method, if a function Y is to be calculated from a set of totally N independent variables, namely X_1, X_2, \dots, X_N , the uncertainty of the function Y can be determined by combining the uncertainties of the individual terms using a root-sum-square method, i.e.

$$\Delta Y = \left[\sum_{i=1}^N \left(\frac{\partial Y}{\partial X_i} \Delta X_i \right)^2 \right]^{1/2} \quad (8)$$

Using the accuracies of the instruments provided in Table 2, the maximum uncertainties of the cooling capacity, compressor power, and COP were found as 0.0516 kW, 0.0529 kW, and 0.0379, respectively.

RESULTS AND DISCUSSION

Comparisons of the various performance merits of the experimental system using R134a and R1234yf are shown in Figures 4–10 as functions of the compressor speed and air temperatures incoming the condenser and evaporator.

The influence of the compressor speed on the conditioned air temperature leaving the evaporator of the AAC system is indicated in Figure 4. The conditioned air temperature drops for both refrigerants with rising compressor speed. When the air temperatures incoming the condenser and evaporator rise simultaneously, the conditioned air temperature increases. For 27°C air inlet temperatures, the AAC system with R1234yf yielded 1.4–3.2°C higher conditioned air temperatures compared to the system with R134a

as a function of the compressor speed. When the air inlet temperatures were 37°C, the system with R1234yf resulted in 1.1–3.5°C higher conditioned air temperatures.

The influence of the compressor speed on the refrigerant mass flow rate is shown in Figure 5. For both refrigerant cases, the refrigerant flow rate gets higher with rising compressor speed and air temperatures incoming the condenser and evaporator. When the incoming air temperatures were 27°C, the R1234yf mass flow rate was 17.4–22.3% higher than the R134a one. Because the specific volume of R1234yf entering the compressor is lower than that of R134a for the same saturation temperature, the compressor circulates R1234yf at a higher rate. When the incoming air temperatures were 37°C, the mass flow rate of R1234yf was 9.3–16.2% higher than that of R134a.

The influence of the compressor speed on the refrigeration capacity is depicted in Figure 6. Since the refrigerant mass flow rate increases with rising compressor speed, the refrigeration capacity gets higher with the compressor speed for both refrigerants as well. Furthermore, rising air

temperature entering the evaporator promotes the heat transfer in this component, thus causing a higher refrigeration capacity. When the air temperatures incoming the evaporator and condenser were 27°C, the system with R1234yf provided 0.4–4.6% lower refrigeration capacity in comparison to the system with R134a. On the other hand, when the air temperatures were 37°C, the R1234yf system yielded 7.8–10.9% lower refrigeration capacities compared to the system with R134a. In comparison to R1234yf, R134a has 21–28% higher latent heat of vapourisation as a function of the saturation temperature [19]. Therefore, the system with R134a provides a higher refrigeration capacity.

The influence of the compressor speed on the compression power is presented in Figure 7. Because the refrigerant flow rate gets higher with rising compressor speed and air temperatures incoming the condenser and evaporator, the compressor power increases with these parameters as well. When the inlet air temperatures were 27°C, the R1234yf system absorbed 2.8–7.1% more compressor power than the R134a one. On the other hand, the system with R1234yf

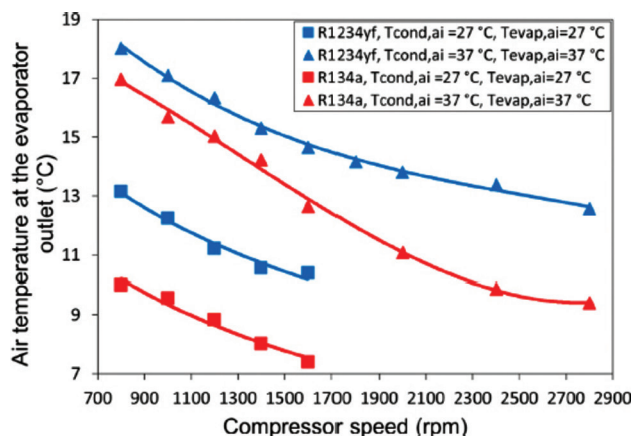


Figure 4. The conditioned air temperature with respect to the compressor speed.

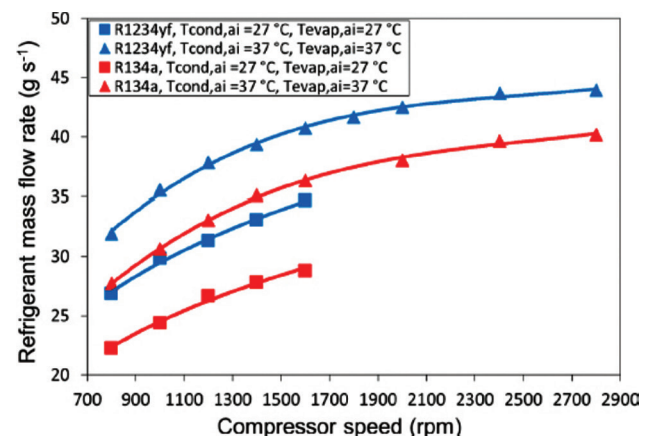


Figure 5. The refrigerant mass flow rate with respect to the compressor speed.

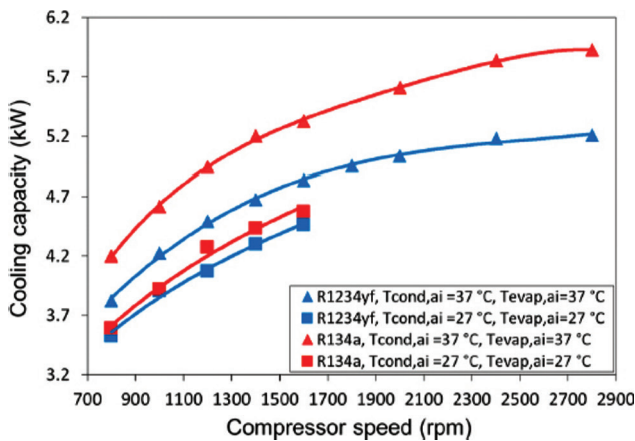


Figure 6. The refrigeration capacity with respect to the compressor speed.

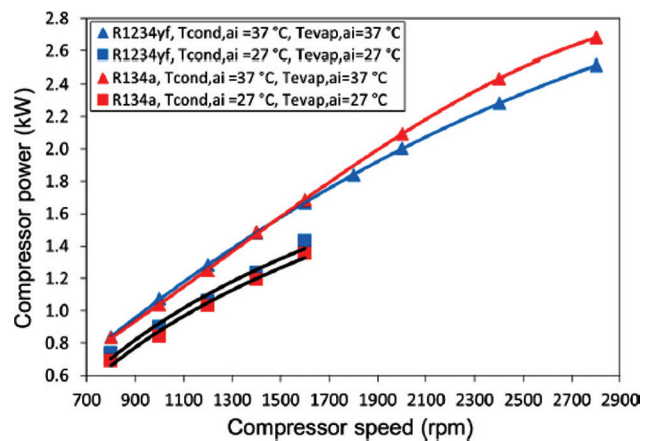


Figure 7. The compressor power with respect to the compressor speed.

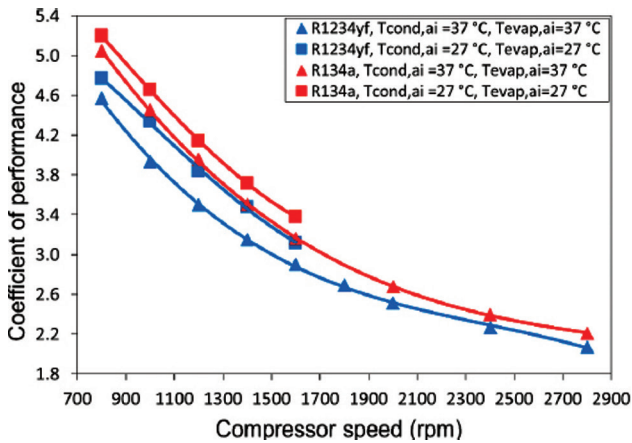


Figure 8. The coefficient of performance with respect to the compressor speed.

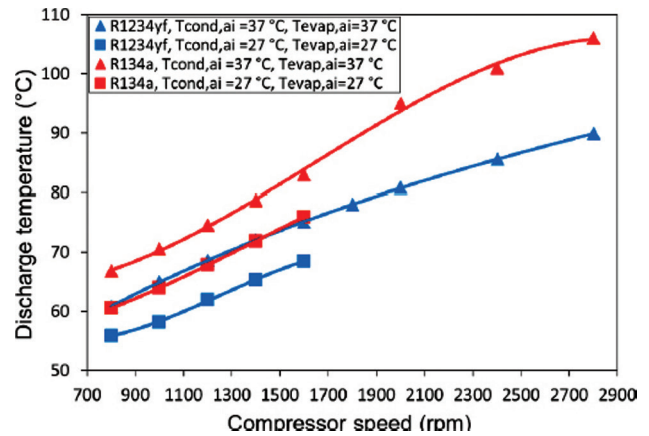


Figure 9. The compressor discharge temperature with respect to the compressor speed.

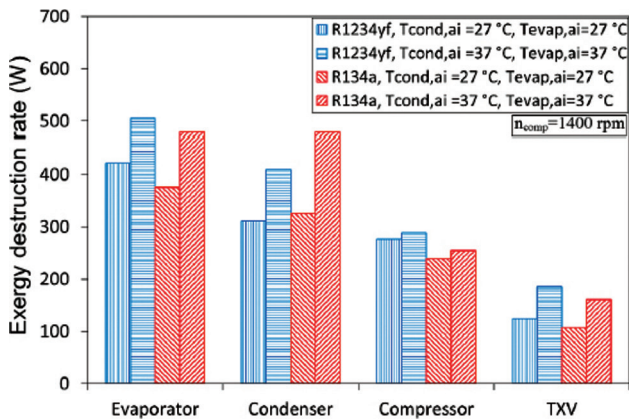


Figure 10. The exergy destruction rates in the components.

required less compressor power after the speed of 1600 rpm when the air temperatures were 37°C. At 2800 rpm, the R1234yf system absorbed on average 6.2% less compressor power than the R134a one.

The COP for the experimental AAC system is indicated in Figure 8. For both refrigerants, the COP drops with rising compressor speed and increasing air temperatures incoming the condenser and evaporator. Even though the refrigeration capacity gets higher with rising compressor speed, the compressor power increases more abruptly than it does. Therefore, the COP for the system gets lower with rising speed. Similarly, as the air temperatures incoming the condenser and evaporator rise, the compression power increases more abruptly than the refrigeration capacity does, thus reducing the COP. When the air inlet temperatures were 27°C, the AAC system with R1234yf yielded 6.4–8.2% lower COP in comparison to the system with R134a, while the R1234yf system resulted in 5.5–11.6% lower COP for 37°C air inlet temperatures.

The influence of the compressor speed on the compressor discharge temperature is shown in Figure 9. This

temperature gets higher with rising compressor speed and air temperatures incoming the condenser and evaporator for both refrigerant cases. Higher discharge temperatures decrease the lifetime of the compressor lubrication oil but promote heat rejection in the condenser, thus reducing the required heat transfer area. For the air inlet temperatures of 27°C and 37°C, the R1234yf system resulted in 4.7–7.4°C and 5.5–16.1°C lower discharge temperatures than the R134a one, respectively.

The exergy destruction rates in the AAC system components are presented in Figure 10 for a sample compressor speed of 1400 rpm. The evaporator caused the highest exergy destruction rate, while the condenser, compressor, and TXV destructed less exergy in decreasing order. The exergy destruction in the evaporator stems from the heat transfer between the air and refrigerant. The higher the temperature difference between these two streams, the larger the exergy destruction rate. Therefore, for both refrigerant cases, operations at the air inlet temperature of 37°C destructed more exergy in comparison to the 27°C operations. In the evaporator, R1234yf yielded 5.2–12.3% more exergy destruction rates than R134a. Similarly, the condenser exergy destruction rates for the air inlet temperature of 37°C were greater than those for 27°C. Because R1234yf results in lower compressor discharge temperatures, the average temperature difference between the refrigerant and airstreams in the condenser are lower for this refrigerant, which yields lower condenser exergy destruction rates in comparison to R134a. According to test results, R1234yf yielded 4.4–14.7% lower condenser exergy destruction rates than R134a. Although R1234yf operates with lower compressor pressure ratios, it causes a higher refrigerant flow rate, thereby causing larger exergy destruction rates in the compressor relative to R134a. It is seen that R1234yf resulted in 13.4–15.8% more compressor exergy destruction rates depending on the air inlet temperature. Since higher air inlet temperatures promote the refrigerant mass

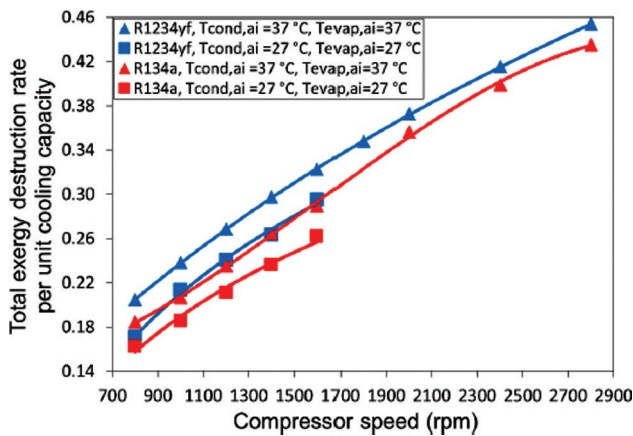


Figure 11. The total exergy destruction rate per unit refrigeration capacity with respect to the compressor speed.

flow rate and compressor pressure ratio, they cause higher exergy destruction rates in the compressor. Finally, mainly due to the increased refrigerant flow rate, R1234yf yielded 15.3–16.7% higher rates of exergy destruction in the TXV.

The influence of the compressor speed on the total exergy destruction rate per unit refrigeration capacity is indicated in Figure 11. As the compressor speed or incoming air temperatures rise, the exergy destruction rates in the components get higher more abruptly than the refrigeration capacity does, thereby leading to elevated total exergy destructions per unit refrigeration capacity. When the temperatures of the incoming air streams were 27°C, the total exergy destruction rate per unit refrigeration capacity of the R1234yf system was 5.2–14.8% larger compared to the R134a system. On the other hand, when the air temperatures were 37°C, the same ratio of the R1234yf system was 4.1–5.3% larger than that of the R134a one.

CONCLUSION

Various performance merits of an AAC system using R1234yf as a replacement for R134a have been investigated. The experimental system was set up in the laboratory by adding mechanical measurement devices to the original AAC system. The values of the system performance parameters were determined with respect to the compressor speed and air stream temperatures incoming the condenser and evaporator. The main results attained in this study are as follows.

- The R1234yf system yielded 0.4–10.9% lower refrigeration capacity than the R134a one. The higher the air temperatures entering the evaporator and condenser, the larger the difference in the refrigeration capacities provided by both systems.
- The R1234yf system resulted in a 5.5–11.6% lower COP relative to the R134a system.

- The R1234yf system yielded 4.7–16.1°C lower compressor discharge temperature in comparison to the R134a system.
- The R1234yf system yielded 1.1–3.5°C higher conditioned air temperatures.
- For both refrigerant cases, the largest exergy destruction occurred in the evaporator, while the condenser, compressor, and TXV caused fewer lower exergy destructions in reducing order.
- The R1234yf system yielded larger evaporator, compressor, and TXV exergy destruction rates, but lower condenser exergy destruction rate relative to the R134a system.
- The R1234yf system yielded a 4.1–15.3% greater total exergy destruction rate per unit refrigeration capacity.

These results suggest that R1234yf can be used as a replacement for R134a at the expense of slight decreases in refrigeration capacity and COP. However, employing a larger evaporator and compressor can compensate for the poor performance of R1234yf in AAC systems.

Future works might be oriented to evaluate the experimental performance of R1234ze, another refrigerant from the HFO group, in AAC systems. Moreover, in order to address energy-efficient heating demand in electric vehicles, the performance of R1234yf in the AAC systems with heat pump feature can be investigated.

NOMENCLATURE

AAC	Automotive air conditioning
AC	Air conditioning
c_p	Specific heat, kJ/kgK
COP	Coefficient of performance
$\dot{E}x_d$	Rate of exergy destruction, kW
GWP	Global warming potential
h	Specific enthalpy, kJ/kg
HFC	Hydrofluorocarbon
HFO	Hydrofluoroolefin
IHX	Internal heat exchanger
\dot{m}	Mass flow rate, kg/s
ODP	Ozone depleting potential
P	Pressure, kPa
\dot{Q}	Heat transfer rate, kW
R	Ideal gas constant, kJ/kgK
s	Specific entropy, kJ/kgK
T	Temperature, K or °C
T_0	Dead state temperature, K
TXV	Thermostatic expansion valve
VCR	Vapour-compression refrigeration
\dot{W}	Power, kW

Greek symbols

ω	Humidity ratio
ψ	Specific flow exergy, kJ/kg

Subscripts

0	Dead state
a	Air
ai	Air inlet
$comp$	Compressor
$cond$	Condenser
cv	Control volume
$evap$	Evaporator
in	Inlet
out	Outlet
r	Refrigerant
tot	Total
v	Water vapour

AUTHORSHIP CONTRIBUTIONS

Concept: A.A., M.H.; Design: A.A., M.H.; Supervision: A.K.; Materials: A.A.; Analysis: A.A.; Literature search: A.A., A.K.; Writing: A.A., M.H.; Critical revision: M.H.

DATA AVAILABILITY STATEMENT

No new data were created in this study. The published publication includes all graphics collected or developed during the study.

CONFLICT OF INTEREST

The author declared no potential conflicts of interest with respect to the research, authorship, and/or publication of this article.

ETHICS

There are no ethical issues with the publication of this manuscript.

REFERENCES

- [1] European Union. Regulation (EU) No 517/2014 of the European Parliament and of the Council of 16 April 2014 on fluorinated greenhouse gases and repealing Regulation (EC) No 842/2006. *Offic J EU* 2014;150:195–30.
- [2] Zhang Z, Wang J, Feng X, Chang L, Chen Y, Wang X. The solutions to electric vehicle air conditioning systems: A review. *Renew Sust Energ Rev* 2018;91:443–63. <https://doi.org/10.1016/j.rser.2018.04.005>.
- [3] Wang CC. System performance of R-1234yf refrigerant in air-conditioning and heat pump system - An overview of current status. *Appl Therm Eng* 2014;73:1412–20. <https://doi.org/10.1016/j.applthermaleng.2014.08.012>.
- [4] Lee Y, Jung G. A brief performance comparison of R1234yf and R134a in a bench tester for automobile applications. *Appl Therm Eng* 2012;35:240–42. <https://doi.org/10.1016/j.applthermaleng.2011.09.004>.
- [5] Navarro-Esbri J, Mendoza-Miranda JM., Mota-Babiloni A, Barragan-Cervera A, Belman-Flores JM. Experimental analysis of R1234yf as a drop-in replacement for R134a in a vapour compression system. *Int J Refrig* 2013;36:870–80. <https://doi.org/10.1016/j.ijrefrig.2012.12.014>.
- [6] Navarro E, Martinez-Galvan IO, Nohales J, Gonzalez-Macia J. Comparative experimental study of an open piston compressor working with R-1234yf, R-134a and R-290. *Int J Refrig* 2013;36:768–75. <https://doi.org/10.1016/j.ijrefrig.2012.11.017>.
- [7] Mota-Babiloni A, Navarro-Esbri J, Barragan-Cervera A, Moles F, Peris B. Drop-in energy performance evaluation of R1234yf and R1234ze(e) in a vapor compression system as R134a replacements. *Appl Therm Eng* 2014;71:259–65. <https://doi.org/10.1016/j.applthermaleng.2014.06.056>.
- [8] Daviran S, Kasaeian A, Golzari S, Mahian O, Nasirivatan S, Wongwises S. A comparative study on the performance of HFO-1234yf and HFC-134a as an alternative in automotive air conditioning systems. *Appl Therm Eng* 2017;110:1091–00. <https://doi.org/10.1016/j.applthermaleng.2016.09.034>.
- [9] Direk M, Kelesoglu A, Akin A. Drop-in performance analysis and effect of IHX for an automotive air conditioning system with R1234yf as a replacement of R134a. *Strojnicki vestnik - J Mech Eng* 2017;63:314–19. <https://doi.org/10.5545/sv-jme.2016.4247>.
- [10] Wantha C. Analysis of heat transfer characteristics of tube-in-tube internal heat exchangers for HFO-1234yf and HFC-134a refrigeration systems. *Appl Therm Eng* 2019;157:113747, 1–10. <https://doi.org/10.1016/j.applthermaleng.2019.113747>.
- [11] Aral MC, Hosoz M, Suhermanto M. Empirical correlations for the performance of an automotive air conditioning system using R1234yf and R134a. *J Therm Sci Tech* 2017;37:127–37.
- [12] Yataganbaba A, Kilicarlan A, Kurtbas I. Exergy analysis of R1234yf and R1234ze as R134a replacements in a two evaporator vapour compression refrigeration system. *Int J Refrig* 2015;60:26–37. <https://doi.org/10.1016/j.ijrefrig.2015.08.010>.
- [13] Cho H, Park C. Experimental investigation of performance and exergy analysis of automotive air conditioning systems using refrigerant R1234yf at various compressor speeds. *Appl Therm*

- Eng 2016;101:30–37. <https://doi.org/10.1016/j.applthermaleng.2016.01.153>.
- [14] Golzari S, Kasaeian A, Daviran S, Mahian O, Wongwiset S, Sahin AZ. Second law analysis of an automotive air conditioning system using HFO-1234yf, an environmentally friendly refrigerant. *Int J Refrig* 2017;73:134–43. <https://doi.org/10.1016/j.ijrefrig.2016.09.009>.
- [15] Devecioglu AG, Oruc V. A comparative energetic analysis for some low-GWP refrigerants as R134a replacements in various vapor compression refrigeration systems. *J Therm Sci Tech* 2018;38:51–61.
- [16] Chopra K, Sahni V, Mishra RS. Energy, exergy and sustainability analysis of two-stage vapour compression refrigeration system. *J Therm Eng* 2015;1:440–44. <https://doi.org/10.18186/jte.95418>.
- [17] Agarwal S, Arora A, Arora BB. Thermodynamic performance analysis of dedicated mechanically subcooled vapour compression refrigeration system. *J Therm Eng* 2019;5:222–36.
- [18] Alkan A. Theoretical and Experimental Investigation of Using R1234yf Instead of R134a in an Automobile Air Conditioning System. Ph.D. Thesis, Sakarya University, Sakarya, Turkey; 2015 (in Turkish).
- [19] Cho H, Lee H, Park C. Performance characteristics of an automobile air conditioning system with internal heat exchanger using refrigerant R1234yf. *Appl Therm Eng* 2013;61:563–69. <https://doi.org/10.1016/j.applthermaleng.2013.08.030>.
- [20] Li Z, Khanmohammadi S, Khanmohammadi S, Al-Rashed AA, Ahmadi P, Afrand M. 3-E analysis and optimisation of an organic rankine flash cycle integrated with a PEM fuel cell and geothermal energy. *Int J Hydrogen Energ* 2020;45:2168–85. <https://doi.org/10.1016/j.ijhydene.2019.09.233>.
- [21] Saadat-Targhi M, Khanmohammadi S. Energy and exergy analysis and multi-criteria optimization of an integrated city gate station with organic Rankine flash cycle and thermoelectric generator. *Appl Therm Eng* 2019;149:312–24. <https://doi.org/10.1016/j.applthermaleng.2018.12.079>.
- [22] Kumar V, Karimi MN, Kamboj SK. Comparative analysis of cascade refrigeration system based on energy and exergy using different refrigerant pairs. *J Therm Eng* 2020;6:106–16. <https://doi.org/10.18186/thermal.671652>.
- [23] Ozgener O, Hepbasli A. Modelling and performance evaluation of ground source (geothermal) heat pump systems. *Energ Build* 2007;39:66–75. <https://doi.org/10.1016/j.enbuild.2006.04.019>.
- [24] Hosoz M, Direk M, Yigit KS, Canakci M, Turkcan A, Alptekin E, Sanli A. Performance evaluation of an R134a automotive heat pump system for various heat sources in comparison with baseline heating system. *Appl Therm Eng* 2015;78:419–27. <https://doi.org/10.1016/j.applthermaleng.2014.12.072>.
- [25] Moffat RJ. Describing the uncertainties in experimental results. *Exp Therm Fluid Sci* 1988;1:3–17. [https://doi.org/10.1016/0894-1777\(88\)90043-X](https://doi.org/10.1016/0894-1777(88)90043-X).